A Vehicle Simulation Model and Automated Driving Features Validation for Low-Speed High Automation Applications

Jose Angel Matute-Peaspan⬤, *Member, IEEE*, Asier Zubizarreta-Pico⬤, and Sergio E. Diaz-Briceno⬤

Abstract— The low-speed high automation (LSHA) is foreseen as a development path for new types of mobility, improving road safety and addressing transit problems in urban infrastructures. As these automation approaches are still in the development phase, methods to improve their design and validation are required. The use of vehicle simulation models allows reducing significantly the time deployment on real test tracks, which would not consider all the scenarios or complexity related to automated driving features. However, to ensure safety and accuracy while evaluating the proper operation of LSHA features, adequate validation methodologies are mandatory. In this study a two-step validation methodology is proposed: Firstly, an open-loop test set attempts to tune the required vehicle simulation models using experimental data considering also the dynamics of the actuation devices required for vehicle automation. Secondly, a closed-loop test strives to validate the selected automated driving functionality based on test plans, also improving the vehicle dynamics response. To illustrate the methodology, a study case is proposed using an automated Renault Twizy. In the first step, the brake pedal and steering wheel actuators' behavior is modeled, as well as its longitudinal dynamics and turning capacity. Then, in a second step, an LSHA functionality for Traffic Jam Assist based on a Model Predictive Control approach is evaluated and validated. Results demonstrate that the proposed methodology is capable not only to tune vehicle simulation models for automated driving development purposes but also to validate LSHA functionalities.

Index Terms— Autonomous vehicles, system validation, predictive models, motion control.

I. INTRODUCTION

THE development of driving automation functionalities has increased over the last decades, increasing their complexity while pushing to adequate the available validation procedures to this breakthrough technology [1]. Advanced Driver

Jose Angel Matute-Peaspan is with the Industry and Transport Division, Tecnalia Research & Innovation, 20009 Donostia-San Sebastian, Spain, and also with the Automatic Control and System Engineering Department, University of the Basque Country (UPV/EHU), 48940 Bilbao, Spain (e-mail: joseangel.matute@tecnalia.com).

Asier Zubizarreta-Pico is with the Automatic Control and System Engineering Department, University of the Basque Country (UPV/EHU), 48940 Bilbao, Spain.

Sergio E. Diaz-Briceno is with the Industry and Transport Division, Tecnalia Research & Innovation, 20009 Donostia-San Sebastian, Spain.

Assistance Systems (ADAS) require a significant amount of track testing hours before they reach the market. Hence, an increased testing effort is expected for a higher level of automation, such as Automated Driving Systems (ADS). To validate ADS, track testing has to be complemented with trials in simulations, to reduce development time and costs [2]. Therefore, well-defined validation methodologies and trustworthy virtual test platforms must be assured [3].

A particular subset of ADS is present in Low-Speed High Automation (LSHA) features, which are related mainly to small (4-15 passengers), low-speed (40km/h of top speed) and automated (SAE Level 4) vehicles. Some examples of LSHA features are Lane-Keeping Assist (LKA), Cruise Control (CC), Adaptive Cruise Control (ACC) and bus-stop automation systems [1]. The spectrum of possible traffic scenarios in LSHA features is reduced to a clear Operative Design Domain (ODD) [4] which permits an easier evaluation of their performance using simulation and track testing [5].

To make use of simulation-based validation approaches both lateral and longitudinal vehicle dynamics to have to be properly modeled and tuned, as in LSHA features both motion controls are required. A generic approach to computational model simulation validation is defined in [6], depicting aspects to consider through validation processes and possible issues related to prediction and model calibration. The proposed classic approach when validating vehicle dynamics models relies on the comparison of experimental and simulation results [7]. As the pure and absolute validation of a simulation model is impossible, it only can be defined as "not invalid" if the difference between a System Response Quantity (SRQ) obtained from simulation (SRQ^p) and experimental measurements (SRQ^m) fulfills a defined validity criterion [2].

Addressing this need of models and proper validation, several studies have been focused on the vehicle dynamics model validation through the so-called validation triangle between standardized test maneuvers, simulation models and real-world [8]. Transient response, fundamental application, and time-domain analysis are part of the methodology. While lateral dynamic validation test maneuvers and methods have been studied in depth [7], proper documentation is still lacking for the longitudinal behavior. A summary of key methods for longitudinal vehicle motion is highlighted in Tab. I.

Based on these, some authors have validated the longitudinal vehicle motion separately [9], [10], although the entire system would be evaluated in a unique test saving time and effort.

TABLE I
SUMMARY OF LONGITUDINAL TEST MANEUVERS AND METHODS

Test maneuver	Characterization Aim	Methods
Straigth-line acceleration [17] [18]	Drive-train performance	- Different test conditions [17] - Pedal Robot or by-wire system [17] - Confidence intervals [18]
Coast-down [17] [10]	Aerodynamic drag and rolling resistance	- Different test conditions - No validation metrics reported
Coast-to-stop on slope [17]	Low speed tire models	- Different test conditions - No validation metrics reported
Straigth-line braking [17] [18] [19]	Braking performance	- Different test conditions [17] [19] - Pedal Robot [17] [19] - Qualitative or quantitative comparison [19] - Confidence intervals [18]
Low speed straight-line [9]	Drive-train braking	- By-wire system - Confidence intervals

Also, note that when considering LSHA features, the required actuator system should also be considered in the vehicle model [11], which most of the cited works ignore [12]–[14]. Moreover, classic test maneuvers may not be representative of conventional driving scenarios in which both lateral and longitudinal motion evaluation is important [15], [16].

Consequently, test cases, data handling, and metrics must be effectively described in vehicle dynamics and automated driving features validation projects [7], [20], [21], trying to obtain the best balance between the effort to gain model confidence and the value to the final user [10], [22].

In this work, a novel two-step validation methodology is proposed. Firstly, an open-loop test procedure allows tuning the vehicle simulation model, including the actuation devices required for implementing the LSHA application. Secondly, a closed-loop test procedure is proposed to test the automated driving features. To illustrate the approach, a study case based on an automated Renault Twizy is detailed, in which a Traffic Jam Assist feature is implemented. This is achieved by a control formulation based on a Model Predictive Control (MPC) that makes use of an adaptive weight-related with lateral accelerations that avoid the use of a speed planner.

The rest of the work is structured as follows. In Section II, the validation approach for vehicle simulation models and LSHA features is described; Section III describes the application of the methodology in a study case considering an automated Renault Twizy; Section IV analyzes thoroughly the validation results obtained. Finally, the main ideas, results and further research underway are summarized in Section V.

II. VALIDATION TEST METHODOLOGY

In this section a validation test methodology inspired on [6] is proposed, which completes the aforementioned validation approach to define vehicle simulation models for developing LSHA features. Then, in Section III, more detail in its implementation in a study case will be given. Note that different from the works cited in Section I, this approach considers also the surrounding sensing, decision-making and low-level control required for developing automated features.

A summary of the proposed validation test methodology is detailed in Fig. 1. The proposed approach is based on two steps. Firstly, an open-loop validation test methodology

is proposed to identify useful parameters of the automated vehicle to assure reliability during simulations, such as time delay, rate limit and control gains of real actuation, as well as the vehicle's capacity to accelerate, brake and turn. Secondly, a closed-loop validation test methodology is proposed that allowing to test and tune vehicle motion control algorithms based on the dynamic model defined in the first step. Moreover, a refinement of the vehicle dynamics model is also possible by using closed-loop tests.

In both approaches, the SRQ difference from simulation predictions and experimental measurements will be used to validate both the simulation models and the decision-making and motion control features. Uncertainty and error calculations are also recommended as a good practice for SRQ difference [7]. Accuracy requisites define the acceptance of the metrics to validate the vehicle model and the automated driving system.

A. Open-Loop Validation Tests

The open-loop validation tests aim to determine the dynamic model of both the vehicle and its internal actuation system so that this model must be feasible enough to time-boost the development of LSHA functionalities through simulations.

The first step in the open-loop validation test methodology is to gather the parameters of interest associated with the test vehicle that are useful to define the vehicle model and the experiment scope. Typical parameters identified in vehicle dynamics modeling are; frontal area, rolling resistance coefficient, locations of the center of gravity, suspension and steering parameters, wheel inertia and tire model [23]. Depending on the desired vehicle model complexity and accuracy more or fewer parameters are required.

In contrast with other methodologies generally used to validate vehicle dynamics model simulations [12]–[14], the actuation behavior on the inputs of the vehicle (steering wheel, throttle, and brake pedals) has a remarkable importance in this work. When considering vehicles with LSHA functionalities, a low-level control layer exists and receives the position commands from the high-level control. Hence, as this low-level control layer influences the dynamics of the inputs and the vehicle, a proper actuation system parametrization is proposed to ensure accuracy in the simulated model.
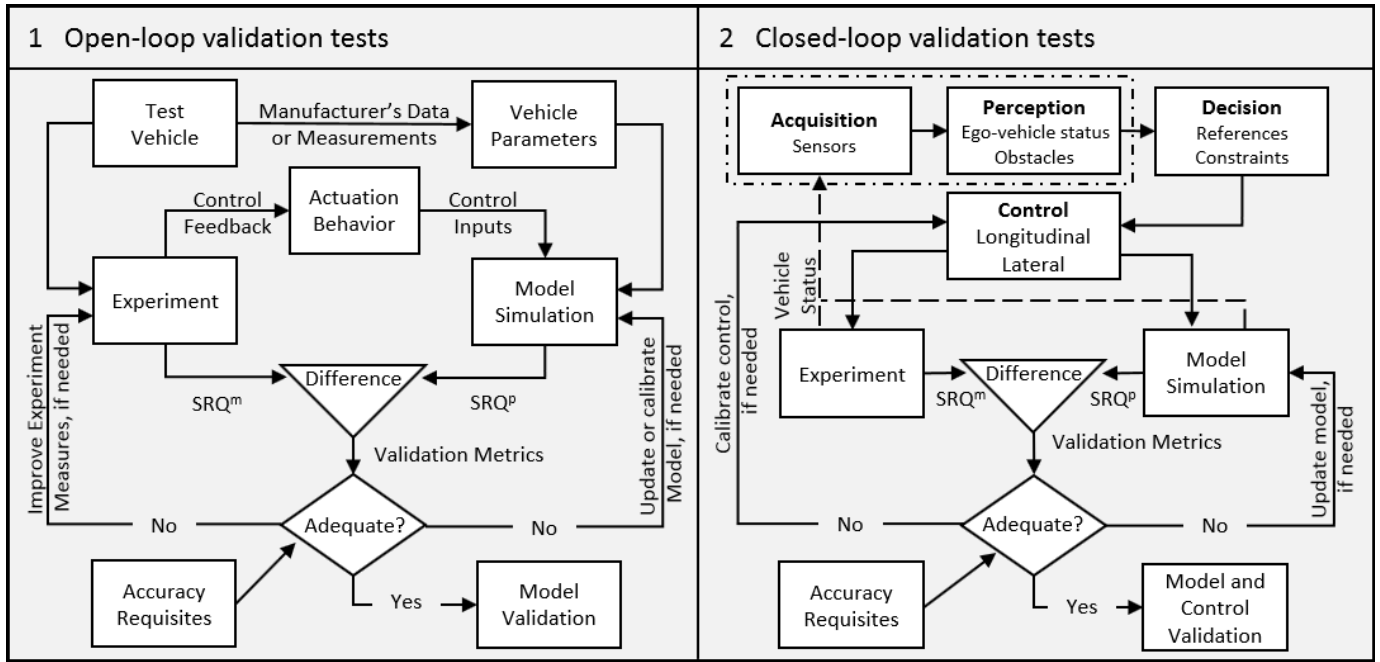
Fig. 1.   Open and closed loop procedures for vehicle model, and decision and control functionalities validation.

Once the actuation behavior and vehicle dynamics are modeled, the SRQ difference is evaluated to conclude whether the model satisfies the accuracy requirements. If the simulation model is considered not valid, either experimental measurements need to be added/improved or the simulation model updated/calibrated [24].

B. Closed-Loop Validation Tests

Once a feasible dynamic model for the vehicle and its internal actuation system is defined, this model can be used to time-boost the development of ADAS/ADS functionalities employing a simulation framework that permits the evaluation of perception, decision-making and/or motion control algorithms.

This way, if an LSHA feature of a certain level of automation is to be tested, the steps defined in Fig 1 are to be followed. The ego-vehicle status and surrounding obstacles are gathered and processed in the Acquisition and Perception stages, respectively. The obtained information from the vehicle and its surroundings is then used in the Decision stage to define a safe and comfortable driving. The trajectory and speed references are then executed by the Control Stage considering a safe distance from obstacles ahead on-route.

As in the open-loop tests, the same surrounding behavior needs to be defined both in the experiment and the simulation environment to compare their SRQ when evaluating their performance within the control architecture. Moreover, tuning the developed simulation model is possible by comparing vehicle dynamic responses from the performed tests to obtain the desired level of accuracy.

III. STUDY CASE: RENAULT TWIZY

To illustrate the application of the methodology proposed in Section II, in this section a particular Case Study will be

Fig. 2.   Renault Twizy U80 on test circuit.

presented. The aim is to obtain a feasible simulation model of an automated Renault Twizy vehicle (Fig. 2) and use it to simulate and tune an LSHA feature.

The selected vehicle is an electric single-seater vehicle for urban mobility which has been adapted for automated driving. For that purpose, a high-performance onboard computer has been implemented in the vehicle, which executes the desired control architecture on MATLAB/Simulink. The main computer sends command signals to a Programmable Logic Controller (PLC) installed on the test vehicle, which is connected to the different actuator controllers. Two MAXON electrical motors-based actuator systems have been implemented to control the steering wheel and brake pedal actuators. The throttle pedal position commands are possible through by-passing the pedal potentiometer and sending pulse-width modulation signals from the PLC to the Engine Control Unit (ECU). A Global Navigation Satellite System and Inertial Navigation System (GNSS+INS) is used to ensure the real-time location of the vehicle. Fig. 3 summarizes the vehicle instrumentation and low-level actuation control system.

A. Open-Loop Validation: Obtaining a Simulation Model

1) Test Vehicle Simulation Model: A multi-body formulation with Dynacar [25], [26] defines the dynamics of a Renault Twizy 80. This model will be implemented in a real-time
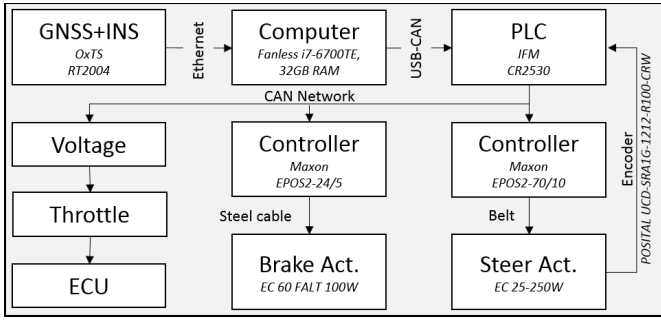
Fig. 3. Test vehicle actuation and instruments for data-acquisition.

TABLE II

VEHICLE TECHNICAL PARAMETERS

Parameter	Value	Unit
Mass	611.50	kg
Dimensions	2.34 x 1.23 x 1.45	m
CG location	-0.93 x 0.00 x 0.49	m
Wheelbase	1.69	m
Track width	1.09	m
Inertia	243.18, 430.17, 430.17	kg-m^2
Front spring stiffness	5840	N/m
Rear spring stiffness	8100	N/m
Front damping	660	N-s/m
Rear damping	1400	N-s/m
Motor	8 (electric)	kW
Traction torque	57	N-m
Transmission ratio	1:9.23	-
Braking torque	360	N-m
Steering:front wheel ratio	1:0.5673	rad
Front wheel radius	0.27	m
Rear wheel radius	0.28	m
Rolling resistance	0.007	-
Drag coefficient	0.64	-

Fig. 4. Actuation models for (a) brake pedal and (c) steering wheel.

TABLE III

ACTUATION PARAMETERS FROM MANUFACTURER

Device	Brake	Steering	Unit
Actuator Model	408057	136210	-
Resistance (R)	3.07e-1	1.43e-1	ohm
Inductance (L_e)	1.88e-4	5.65e-5	H
Rotor inertia (J)	1.21e-4	2.09e-3	kg-m^2
Torque Constant (K_m)	5.34e-2	3.28e-2	N-m/A
Mechanical time (t_m)	1.3e-2	3.99e-1	s

In addition to the aforementioned blocks, the parameters associated with the power-train and braking performance, as well as the angle ratio between the steering wheel and front wheels is obtained from the manufacturer specifications of these elements.

Next, a series of tests will be proposed to validate the simulation model considering the aforementioned elements. The results for these tests will be analyzed in Section IV.

Note that this is an iterative process in which several tests will be required to optimize the model and its parameters to fit experimental data, as some phenomena (as time delays or nonlinear effects) are difficult to model otherwise.

a) Brake and steering actuation: A series of step input commands of different amplitudes will be used to identify the maximum speed and displacement range of each actuator. Additionally, the tuned PID parameters can be extracted from the motor controller to simulate them and optimize the proposed actuation models using experimental tests. The motor positioning will be used as a validation metric to compare the SRQ from measurements and predictions.

b) Longitudinal dynamics: Straight-line acceleration and braking tests are usually employed to characterize longitudinal performance in vehicle dynamics (Tab. I). In this work, however, instead of making different isolated tests, a combined acceleration-braking test is proposed, in which a series of step input commands with similar magnitudes for acceleration and braking is executed, together with intervals of zero input commands. This allows optimizing the power-train and braking parameters, and the aerodynamic drag and rolling resistance constants with the same test results. The acceleration (a_x) and velocity (v_x) will be used as validation metrics.

c) Turning at constant speed: To define the relationship between the steering wheel and front wheel angles, tests with different turning angles at low (1 m/s) constant speed will be executed. This will allow comparing the circular paths described by the test vehicle and simulation model. A localization device is necessary for the development of this

vehicle simulation environment that allows us to test different driving scenarios [26]. The main vehicle technical parameters are presented in Tab. II.

2) Actuation Behavior: As defined in Fig. 3, two electro-mechanical actuator systems are introduced in the brake pedal and steering wheel. Both actuation systems have their low-level controller to ensure that the motors follow the position command given by the high-level controller. The elements that compose the low-level actuation system model are detailed in Fig. 4

As both actuators are electric motors, they can be modeled as second-order transfer functions [27], defined in Eqs. 1a-1d.

$$G(s) = (1/K_e)/(\tau_m \tau_e s^2 + \tau_m s + 1) = W(s)/V(s) \quad (1a)$$

$$\tau_m = R J/(K_e K_t) \quad (1b)$$

$$\tau_e = L_e/R \quad (1c)$$

$$K_e = R J/(t_m K_m) \quad (1d)$$

The motors' parameters have been extracted from the manufacturer (Maxon), and their values are depicted in Tab. III.

Additionally, as in real implementations, a controller is employed to position the device in the desired value with zero error. Moreover, the time delay of the vehicle's internal communications, the rate limit of actuators and the gains for the PID controllers are optimized by-hand through experiments.

3) Model Validation: Once defined the models of the actuation system and the vehicle dynamics, the overall simulation model needs to be validated using experimental data.
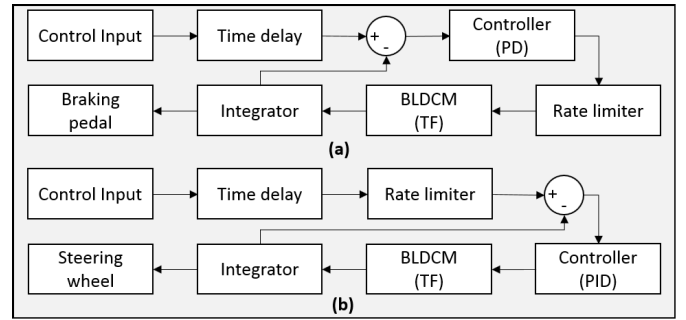
test. The path radius is used as a validation metric. The results for these tests will be shown and analyzed in Section IV.

B. Closed Loop Validation: LSHA Feature Simulation

The proposed methodology allows the testing of LSHA functionalities based on the simulation model obtained previously. As stated earlier, a proper simulation model can be used to time-boost the development of LSHA features, and even further optimize the developed model by a proper choice of closed-loop testing.

In this section, an ADS feature [4] has been selected as a study case. The developed LSHA functionality is a Traffic Jam Assist function that aims to follow a traffic flow at low speeds (<30km/h) without lane change support [1]. To implement this functionality a Model Predictive Control (MPC) approach which combines lateral and longitudinal vehicle motion control will be used. The lateral control allows the vehicle to remain within its lane, while the longitudinal control either maintains the required speed (Cruise Control-CC) or adapts its longitudinal speed to maintain a safe distance from an obstacle or a preceding vehicle (Adaptive Cruise Control-ACC).

In this work, relative distances and velocities concerning the ego-vehicle are defined mimicking a traffic jam situation with a vehicle ahead. The start and finish point of the route as well as the simulated lead-vehicle longitudinal velocity are depicted in Fig. 5. Relative errors below 10% will be considered accurate enough for the model simulation.

1) Decision Stage: The developed functionality is based on an MPC approach that requires relative distance and velocity, location, orientation, and speed limit references to operate properly.

This way, first a vehicle motion planning is required, which defines the overall trajectory and speed references for the desired route. Using this data, location and orientation references $(X_{ref}, Y_{ref}, \psi_{ref})$ necessary for proper performance of the lateral motion control will be defined. Similarly, a speed reference v_x for the longitudinal motion control must be defined in terms of the maximum allowable speed of the road. Moreover, as safety and comfort are an important issue to be considered, an adaptive weight in terms of the vehicle's lateral acceleration (a_y) is used to reduce the speed of the vehicle when taking turns.

Moreover, as the longitudinal vehicle motion control is enabled to switch between CC and ACC modes in the presence of preceding vehicles or obstacles, a proper algorithm to switch between both modes is required.

a) Vehicle motion planning: The trajectory and speed references are defined as detailed in [11]. Bezier curves are employed to smooth the trajectory of a desired route and performing usual maneuvers in urban environments [28].

An ordered list of way-points related to each maneuver is then calculated to provide essential information from the route as location coordinates and orientation (X, Y, ψ). As in urban environments, a value for the longitudinal speed v_x is then specified as the speed limit (v_x^{max}) of the route (5m/s). The route used both for experiment and model simulation is shown in Fig. 5a.
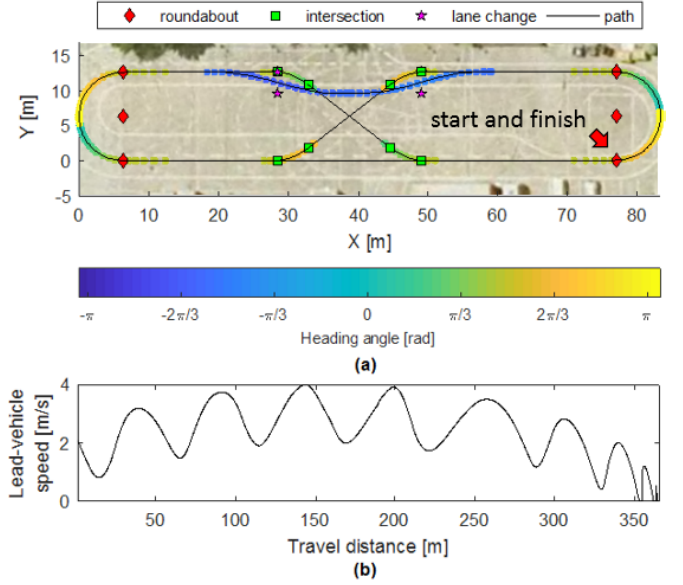

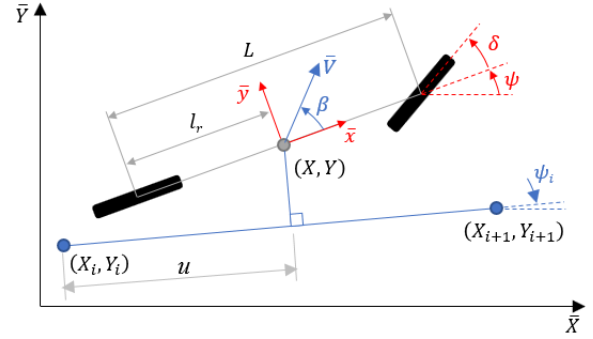Fig. 5. (a) Route and (b) lead-vehicle speed for experiment and simulation.

Fig. 6. Kinematic bicycle model for vehicle motion control.

It is important to remark that the planned route has a path radius magnitude lower than expected in real urban scenarios (<7m). This route is generated considering the space available for real test development.

b) Location and orientation references: A dot product is employed to project X and Y onto one of the consecutive straight segments that describe the route defined in Sec. III-B1a. The bounds of the current segment (u) are defined by the starting (X_i, Y_i) and ending (X_{i+1}, Y_{i+1}) points depicted in Fig. 6. If the projection results in outbounds, a previous or next segment must be selected repeating the estimation procedure. When an in-bounds result is obtained $(0 < u < 1)$, the values for X_{ref}, Y_{ref} and ψ_{ref} are computed from the selected segment. The lateral and angular errors (e_y, e_ψ) can be calculated if needed. The trigonometry is important in the sideslip angle (β) estimation since a path radius is expected from the motion planning as is shown in Eq. 2 [29].

$$\beta = \tan^{-1}(l_r \tan \delta)/L \qquad (2)$$

where l_r is the distance from the rear axle to the CG. The procedure to select the correct segment is detailed in Algo. 1

c) Adaptive weight for safety: An important contribution of this work is the use of an adaptive weight S to modify the driving task in real-time by considering the measured and

---

Algorithm 1 Location and Coordinate References Estimations

Data: Vehicle's states (X, Y, ψ, δ) and planned route information (list of way-points)

Result: Location and orientation references (X_{ref}, Y_{ref}, ψ_{ref}), Lateral and angular errors (e_y, e_ψ)

initialization;

$d_x = X_{i+1} - X_i$; $d_y = Y_{i+1} - Y_i$;

$R_x = X - X_i$; $R_y = Y - Y_i$;

$u = (R_x d_x + R_y d_y) / (d_x^2 + d_y^2)$;

while *u < 0* **do**

  | % select the previous segment;

  | i = i - 1;

  | % calculates u;

end

while *u > 1* **do**

  | % select the next segment;

  | i = i + 1;

  | % calculates u;

end

% references estimation;

$X_{ref} = X_i + (R_x d_x + R_y d_y) d_x / (d_x^2 + d_y^2)$;

$Y_{ref} = Y_i + (R_x d_x + R_y d_y) d_y / (d_x^2 + d_y^2)$;

$\psi_{ref} = \psi_i$;

% lateral and angular error estimation;

$e_y = (R_y d_x + R_x d_y) / \sqrt{d_x^2 + d_y^2}$;

$e_\psi = \psi - \psi_i$;

---

predicted lateral acceleration (a_y).

$$S = 1 - C_w \, a_y^2 / a_y^{max} \qquad (3)$$

where $C_w = 4$, and is manually tuned. a_y can be predicted using the path radius ($R = L/\tan\delta$), from the front wheel steering angle (δ), the wheelbase longitude (L) and the v_x,

$$a_y = v_x^2 \tan\delta / L \qquad (4)$$

Note that S varies from 1 (zero lateral acceleration) to 0 (for high lateral acceleration). Therefore, by considering this adaptive weight in the cost function, the longitudinal speed v_x can be modified to ensure passengers' comfort. This is, for low lateral accelerations, the cost function prioritizes the longitudinal lead-speed; when turning, the acceptable lateral acceleration is prioritized over the set lead-speed.

This is an alternative to the usual off-line speed planning calculation required as a reference for the longitudinal vehicle motion control [11].

d) Longitudinal motion mode switching: The strategy to switch from CC to ACC when needed is based on the relationship between the relative distance (d_r) and velocity (v_r) measurements from the ego-vehicle to a preceding one [29]. This way, the diagram defined in Fig. 7 is used to define the operation mode for the longitudinal vehicle motion control depending on the measured relative distance and speed.

The 'cruise' zone allows to drive in CC mode and the vehicle's v_x is adapted to the v_x^{max} defined in the motion planning section. If a preceding vehicle/obstacle is detected the system switches to ACC mode according to the operation zone where three internal features are available:

- 'speed': v_x is adapted to obtain $v_r = 0$.
- 'head-way': v_x is adapted for $d_r = d_{ref}$.
- 'too-close': $d_r = d_{ref}$ at maximum deceleration.

The reference distance (d_{ref}) is estimated as,

$$d_{ref} = d_r^{min} + v_r \, t_{hw} \qquad (5)$$

where a constant head-way time (t_{hw}) equal to 1s is considered, being this one of the most employed techniques for spacing in car-following [30]. The slope of the line to switch among ACC internal features is defined as,

$$T = -\sqrt{(d_r^{max} - d_r^{min})/(2D)} \qquad (6)$$

where d_r^{max} is the maximum relative distance measured by the sensor, d_r^{min} is the minimum safety distance, and v_r^{max} is the maximum relative speed, in which collision avoidance is preferred instead of a convoy behavior. The deceleration (D) vary among coasting, 'head-way' and 'too-close' modes. These values are defined in Sec. III-B2d. The procedure for longitudinal motion mode switching is detailed in Algo. 2.

Algorithm 2 Longitudinal Motion Operation Mode Switch

Data: Relative distance and velocity (d_r, v_r), adaptive weight (S), slope to switch (T), maximum and minimum relative distance and velocity measurable from sensor (d_r^{max}, d_r^{min}, v_r^{max}), deceleration (D)

Result: Longitudinal motion operation mode

initialization;

if $d_r > d_r^{max}$ *or* $v_r > v_r^{max}$ **then**

  | 'cruise' control armed;

else

  | **if** $d_r > d_r^{min} + Tv_r$ **then**

    | 'speed' control armed;

  | **else**

    | **if** $d_r > d_r^{min} + v_r^2 / (2D)$ **then**

      | 'head-way' control armed;

    | **else**

      | 'too-close' control armed;

    | **end**

  | **end**

end

---

2) Control Stage: In this section, the lateral and longitudinal vehicle motion control approaches based on MPC are detailed in-depth.

a) Vehicle model: MPC approaches require a dynamic model that mimics the behavior of the controlled system to make predictions. To perform a Traffic Jam Assist functionality, the developed MPC requires a lateral and longitudinal vehicle model, a vehicle motion control, and a limited Object an Event Detection and Response (OEDR) model.

The lateral vehicle motion control is performed using a kinematic bicycle model as shown in Fig. 6. The rate of
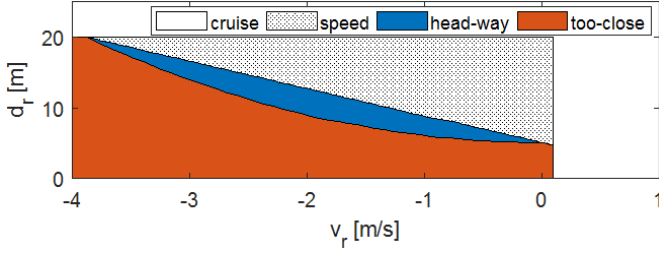
Fig. 7. Diagram for longitudinal motion switching.

Fig. 8. (a) Brake pedal and (b) steering wheel actuation response.

change of the front wheel steering angle ($\Delta\delta$) defines a desired comfort level in the driving task.

The longitudinal vehicle motion control is performed using an integrator model as depicted in Eqs. 7e-7f. The kinematics of the vehicle is modeled as an ideal particle traveling along the route. The longitudinal acceleration (a_x) and jerk (j_x) permit to define a desired level of comfort in the driving task.

The model for a limited OEDR is defined in Eqs. 7g-7h. It modifies the longitudinal vehicle motion control if an object is detected ahead along the predefined route. This strategy strongly depends on the velocity (v_r) and acceleration (a_r) relative to the obstacle ahead.

The lateral jerk ($\dot{a}_y$) presented in Eq. 7i is obtained from the time derivative of Eq. 4. The prediction of a_y is required to modify the magnitude of S described in Eq. 3.

$$\dot{X} = v_x \cos(\psi + \beta) \tag{7a}$$
$$\dot{Y} = v_x \sin(\psi + \beta) \tag{7b}$$
$$\dot{\psi} = v_x \cos\beta \tan(\delta)/L \tag{7c}$$
$$\dot{\delta} = \Delta\delta \tag{7d}$$
$$\dot{v}_x = a_x \tag{7e}$$
$$\dot{a}_x = j_x \tag{7f}$$
$$\dot{d}_r = v_x^{lead} - v_x \tag{7g}$$
$$\dot{v}_r = a_x^{lead} - a_x \tag{7h}$$
$$\dot{a}_y = (2a_x\delta + v_x\Delta\delta/\cos^2\delta)v_x/L \tag{7i}$$

b) MPC formulation: Using Eqs. 7a-7i, the MPC control law can be defined as,

$$\min_{\eta(\cdot),u(\cdot)} \sum_{k=1}^{H} \|\eta_k - \eta_k^{ref}\|_Q^2 + \|u_k\|_R^2 \tag{8a}$$
$$s.t. \ \chi_{k+1} = f(\chi_k, u_k) \tag{8b}$$
$$\chi_f^{min} \leq \chi_k \leq \chi_f^{max} \tag{8c}$$
$$u_f^{min} \leq u_k \leq u_f^{max} \tag{8d}$$

where the cost function (Eq. 8a) penalizes the tracking of the desired outputs $\eta = [\dot{X}, \dot{Y}, \dot{\psi}, \dot{v}_x, \dot{d}_r, \dot{v}_r]$, and the control inputs $u = [\dot{j}_x, \Delta\delta]$ over the sliding horizon H. In order to tune the controller, the weight matrices Q and P are used.

The state variables of the simulation model (Eqs. 7e-7f) $\chi = [\dot{X}, \dot{Y}, \dot{\psi}, \dot{\delta}, \dot{v}_x, \dot{a}_x, \dot{d}_r, \dot{v}_r; \dot{a}_y]$ and u are estimated at each time step k by the nonlinear model f in the Eq. 8b. The sequence for the solution is settled in as $h = t, \ldots, t + H$. The constraints for χ and u are defined in Eqs. 9a-9f.

c) MPC weighting matrices: The weights for the lateral states (X, Y, ψ) remain constant at their maximum value (1)
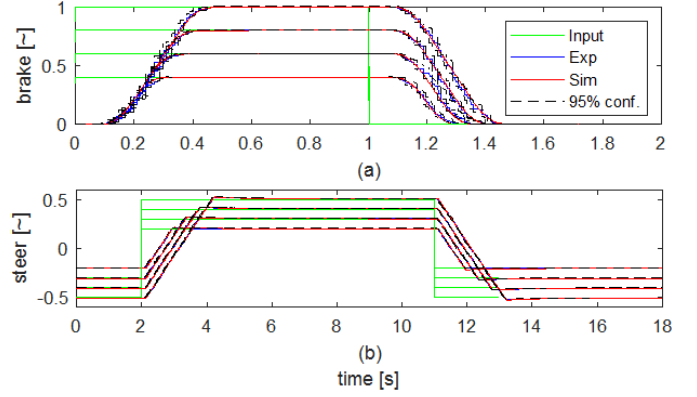
during the driving task, while the weights for the longitudinal ones (v_x, d_r, v_r) vary with S as detailed in Eq. 3 depending on the longitudinal motion mode switching:

- 'cruise': Q = diag([1, 1, 1, S, 0, 0]).
- 'speed': Q = diag([1, 1, 1, 0.1S, S, 0]).
- 'head-way' or 'too-close': Q = diag([1, 1, 1, 0, 0, S]).

This way, the vehicle's location and orientation becomes more important as a_y increases, as the weights of the longitudinal states (v_x, d_r, v_r) decrease their values in comparison with the weights for the lateral states (X, Y, ψ).

The weight of the control inputs ($j_x, \Delta\delta$) are also dependent on S. Thus, they also decrease with the increment of a_y, which allows higher change rates on the input signals meaning a faster input for actuation devices (R = diag([S, S])).

d) MPC constraints: The bounds for χ and u are defined considering the physical capabilities of the actuation devices and the test vehicle that can be found through methods described in Sec.II-A, as well as safety and comfort considerations for the final user. The selected constraint values are:

$$-D < a_x < 0.25m/s^2 \tag{9a}$$
$$-0.50m/s^3 < j_x < 0.50m/s^3 \tag{9b}$$
$$-0.50rad < \delta < 0.50rad \tag{9c}$$
$$-0.50rad/s < \Delta\delta < 0.50rad/s \tag{9d}$$
$$5m < d_r < 20m \tag{9e}$$
$$-2m/s^2 < a_y < 2m/s^2 \tag{9f}$$

where the D constraint value depends on the longitudinal motion operation mode; 'cruise' and 'speed' (D = 0.5m/s²), 'head-way' (D = 1m/s²), and 'too-close' (D = 3m/s²).

e) MPC solver and real-time implementation: The MPC is solved using the open-source ACADO Toolkit [31]. The problem is approximated to a Non-Linear Program (NLP) using the direct multiple shooting as a discretization method and is solved using a Sequential Quadratic Program (SQP) algorithm with a Gauss-Newton iteration. The linear algebra solver qpOASES3 computes the SQP. An Implicit Runge-Kutta of Gauss-Legendre integrator of 2nd order is used to simulate the system in MATLAB/Simulink environment. A horizon $H = 10$ is selected with 0.3s of time discretization.
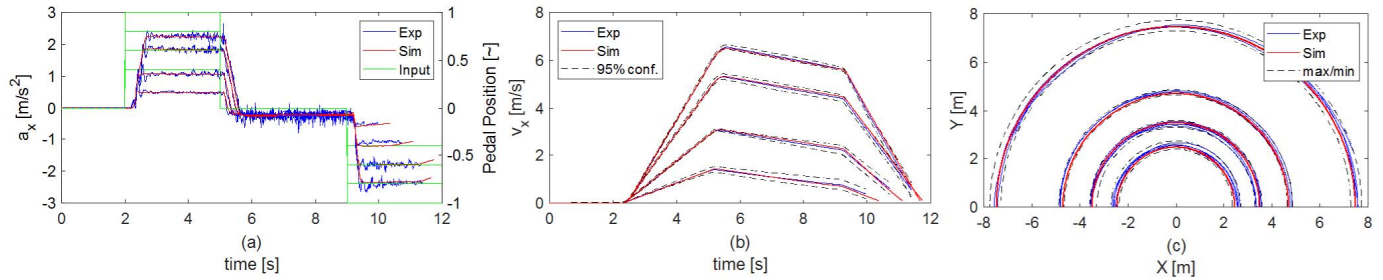
Fig. 9. Results for longitudinal (a) acceleration and (b) velocity from control input to pedals, and (c) turning at constant speed trajectories.

TABLE IV
ACTUATION PARAMETER IDENTIFICATION

Device	Throttle	Brake	Steering	Unit
Time delay	0.1-0.2	0.08	0.08	s
Rate limiter	2.3-2.5	2	0.485	rad/s
Proportional (P)	-	1	0.8	-
Integral (I)	-	0	0.6	-
Derivative (D)	-	0.012	0.2	-
Filter Coefficient	-	100	100	-

IV. RESULTS AND DISCUSSIONS

A. Brake and Steering Actuation Test

Fig. 8 shows comparisons between open-loop model predictions and experimental measurements for brake pedal and steering wheel actuators. As the SRQ (positions) accuracy of the predictions is well within bounds, the actuation models of Fig. 4 (including low-level controllers and mechanical actuators) are considered validated for both brake pedal and steering wheel. Table IV shows the tuned parameters. The results evidence the significant effect of the actuation dynamics on the inputs of the vehicle dynamics.

B. Longitudinal Dynamic Test

Following the scheme of Fig. 1, open-loop tests are performed by the application of a sequence of accelerator and brake pedal step inputs, covering acceleration, coasting, and braking, from a standing, still start to a final full stop. Fig. 9a shows experimental and predicted longitudinal acceleration for four individual tests ranging from 30% to 100% pedal step inputs. The dynamic model is shown to predict well the delays, ramps and acceleration levels obtained in the vehicle. It is noted that, after performing the tests, it was established that the brake pedal was not fully released for a zero input. This fact was considered in the simulations. Fig. 9b shows the corresponding speed profiles, averaged over eight tests for each pedal step size, with their corresponding uncertainty intervals. As the differences between the two SRQs selected (i.e., longitudinal acceleration and speed) are well within bounds, the longitudinal dynamics modeling, coupling vehicle dynamics, and actuators, is considered validated.

C. Turning at Constant Speed Test

Fig. 9c shows steady-state paths for four steering wheel positions (40, 60, 80, and 100%) at a constant speed of 1m/s. Experimental trajectories correspond to the average of eight tests and show their corresponding uncertainties. Note that

only half of the circular trajectories are being plotted so that experimental uncertainties and differences with model predictions can be observed. These open-loop results, comparing measured and predicted path radiuses, validate the steady-state lateral dynamics behavior of the model, allowing tuning of the corresponding parameters, such as the steering wheel/front-wheel angle gain at 12.43/1.

D. LSHA Functionality Test

The Traffic Jam Assist feature previously described is implemented to follow a vehicle with a composed sinusoidal speed profile along the route detailed in Fig. 5b. The SRQ difference depicted in Figs.10-11 are evaluated to validate the model. The same MPC formulation law is used to control the physical vehicle and the simulated model, with the simulation replicating the same track and lead-vehicle motion.

Figs. 10a-b compare the high-level commands to the actuators. Even though small differences at the beginning of the test can propagate and produce qualitative differences, later on, both simulated pedals and steering wheel behavior follow the overall behavior of the experimental measurements. Note that a high-frequency oscillation is present on the brake pedal (both for simulation and experiments). This is related to a small misalignment on the vehicle suspension and the previously analyzed brake pedal issue.

Figs. 10c-d show that the lateral accelerations are very similar along the track, which is reflected also in the S-weight parameter (Fig. 10l), which is derived from the lateral acceleration. Note that the computation of S amplifies the measurement noise in the lateral acceleration, but the effective value follows the simulated values.

The longitudinal acceleration, just as the pedal actuators, follows the same trend and shows the high-frequency component, with some qualitative differences related to small differences in the time at which the lead-vehicle is detected. This is particularly evident in Figs. 10e-f, where the zones at which the lead-vehicle is within the radar reach are plotted. A small difference in the detection time leads to differences in switching the control mode, which carries on to further differences in the switching locations downstream. These differences are not unlike the ones obtained over different experimental runs. The relative distance and speed to the lead-vehicle, as recorded by the on-board radar, evidence how a small-time difference on the radar detection time can affect the ensuing motion (Figs. 10g-h).

The ego-vehicle longitudinal speed depicted in Fig. 10k shows the dynamic response of the model and the physical
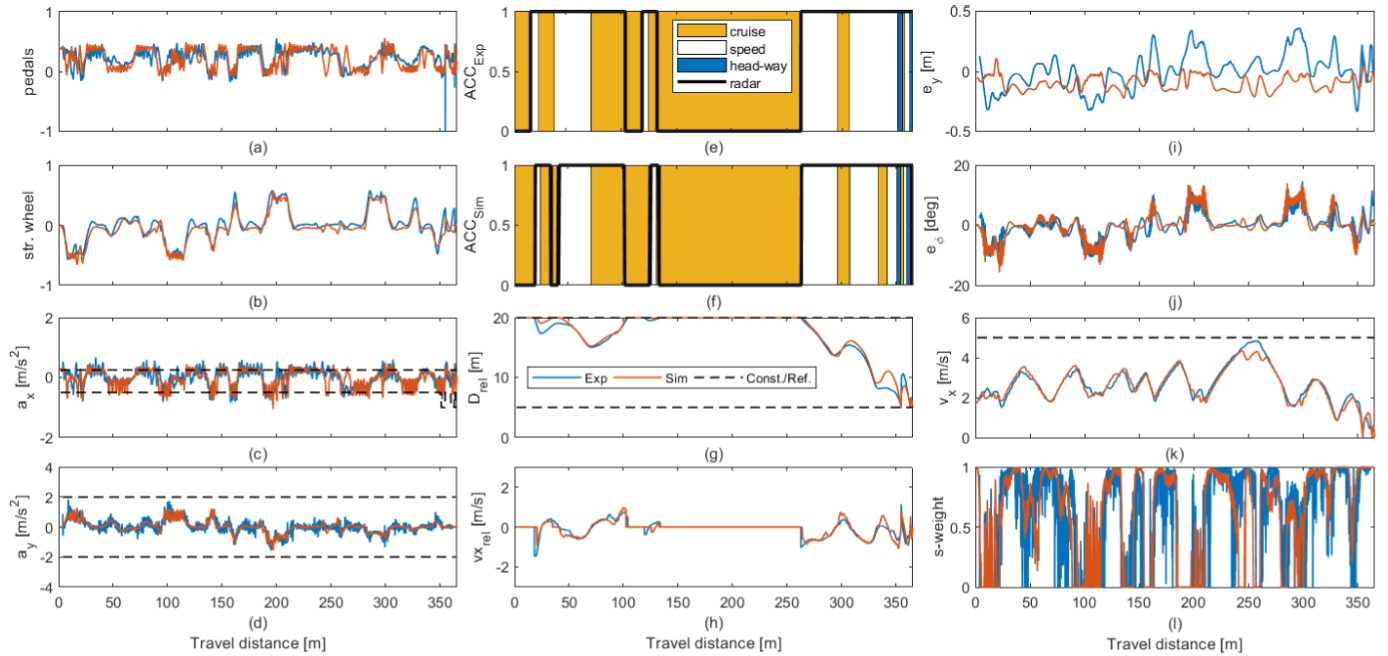
Fig. 10. Results for simulation and experimental tests; control inputs to (a) pedals and (b) steer, (c) longitudinal and (d) lateral accelerations, longitudinal motion operation mode in (e) simulation and (f) experiment, relative (g) distance and (h) velocity during in ACC, (i) lateral and (j) angular errors, (k) longitudinal velocity and (l) adaptive weight variation.
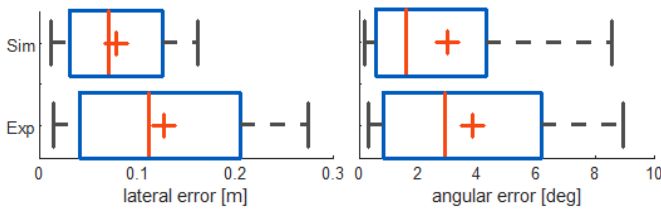

Fig. 11. Lateral and angular errors statistics.

car to be very similar on accelerating and braking, even if it also evidences the difference on the head-way related to control mode switch timing differences.

The lateral and angular errors compiled in Fig. 10i-j evaluate the ability of the control to follow the predefined path. As the same control is applied to both experiments and simulations, the analysis of these errors supports the feasibility of the dynamic model to evaluate or develop control schemes. Experimental and simulated tracking errors show similar behaviors, with the same frequency components, though, as expected, the experiments evidence slightly higher amplitudes, as reflected also in Fig. 11. Further simulation analysis showed that an important component of the tracking errors corresponds to a frequency of around 0.13 Hz, which has been directly related to the control performing compensations to the suspension misalignment. Yet, the model can simulate the actual system even in this condition. In both virtual and real tests the MPC solver achieved a mean solving time below 1ms, being this appropriate for real-time implementations running at 10ms of time step. These analyses were executed on the computer depicted in Fig. 3.

V. CONCLUSION

Low-Speed High Automation (LSHA) features are the basis for new types of mobility in urban environments, existing an increased interest in their developments. However, their testing and validation requires a well-defined validation methodology based on the combination of track and simulation tests. Although several studies have focused on this issue, there is still a lack of a clear specification for the methodology. Moreover, issues regarding the automated features, such as the low-level control, or their influence on the classic track tests, are not considered in most of them.

Hence, in this work, a two-step methodology is proposed to validate not only the vehicle and its actuation models under simulation environments but also LSHA functionalities. For that purpose, first, a set of open-loop tests are proposed, which allow to tune models for the actuation devices, longitudinal and lateral dynamics. Second, the developed model allows us to test LSHA functionalities in a set of closed-loop tests.

To illustrate the approach, a study case based on a Renault Twizy is proposed. In the first step, the vehicle model and its low-level control architecture is validated using real data. Results show that the actuation dynamics has a significant effect that must be considered. In a second step, a MPC based Traffic Jam Assist functionality is tested. The consideration of the lateral acceleration and an adaptive weight in the cost function allows adapting the linear speed to ensure safety and comfort while eliminating the need for a speed planer. The behavior comparison between experiments and simulations demonstrates the validity of the approach.

In conclusion, the proposed validation procedure permits to tune reliable simulated test platforms and automated driving strategies in simulation environments reducing the time on real test implementations. Future works will consider the integration of sensors in closed-loop tests, both in simulation and real vehicle implementation. Furthermore, test platforms of bigger sizes as city buses for LSHA

applications will be considered in association with local manufacturers.

REFERENCES

[1] E. Ertrac and E. Snet, "Ertrac automated driving roadmap," ERTRAC Work. Groups, Brussels, Belgium, Tech. Rep. version 7.0, 2017.

[2] M. Campbell, M. Egerstedt, J. P. How, and R. M. Murray, "Autonomous driving in urban environments: Approaches, lessons and challenges," *Phil. Trans. Roy. Soc. A, Math., Phys. Eng. Sci.*, vol. 368, no. 1928, pp. 4649–4672, Oct. 2010.

[3] P. Heidl and W. Damm, "Highly automated systems: Test, safety, and development processes," SafeTRANS Work. Group, New Delhi, India, Tech. Rep., 2017.

[4] *Taxonomy and Definitions for Terms Related to Driving Automation Systems for on-Road Motor Vehicles*, Standard J3016_201806, SAE Int., Warrendale, PA, USA, 2017.

[5] *Status Report. Special Issue: Autonomous Vehicles*, IIHS-HLDI, CITATION, Chicago, IL, USA, 2018, vol. 53, no. 4.

[6] W. Oberkampf and C. Roy, *Verification and Validation in Scientific Computing*. Cambridge, U.K.: Cambridge Univ. Press, 2010.

[7] E. Kutluay and H. Winner, "Validation of vehicle dynamics simulation models—A review," *Vehicle Syst. Dyn.*, vol. 52, no. 2, pp. 186–200, Feb. 2014.

[8] E. Kutluay, *Development and Demonstration of a Validation Methodology for Vehicle Lateral Dynamics Simulation Models*. Düsseldorf, Germany: VDI-Verlag, 2013.

[9] R. Pastorino, E. Sanjurjo, A. Luaces, M. A. Naya, W. Desmet, and J. Cuadrado, "Validation of a real-time multibody model for an X-by-wire vehicle prototype through field testing," *J. Comput. Nonlinear Dyn.*, vol. 10, no. 3, May 2015, Art. no. 031006.

[10] K. Massow and I. Radusch, "A rapid prototyping environment for cooperative advanced driver assistance systems," *J. Adv. Transp.*, vol. 2018, pp. 1–32, 2018.

[11] J. A. Matute, M. Marcano, A. Zubizarreta, and J. Perez, "Longitudinal model predictive control with comfortable speed planner," in *Proc. IEEE Int. Conf. Auto. Robot Syst. Competitions (ICARSC)*, Apr. 2018, pp. 60–64.

[12] G. J. Heydinger, W. R. Garrott, J. P. Chrstos, and D. A. Guenther, "A methodology for validating vehicle dynamics simulations," *SAE Trans.*, vol. 99, pp. 126–146, Jan. 1990.

[13] W. R. Garrott *et al.*, "Methodology for validating the national advanced driving simulator's vehicle dynamics (NADSdyna)," *SAE Trans.*, vol. 106, pp. 882–894, Jan. 1997.

[14] O. Polach and J. Evans, "Simulations of running dynamics for vehicle acceptance: Application and validation," *Int. J. Railway Technol.*, vol. 2, no. 4, pp. 59–84, 2013.

[15] G. J. Heydinger, C. Schwarz, M. K. Salaani, and P. A. Grygier, "Model validation of the 2006 BMW 330i for the national advanced driving simulator," SAE, Warrendale, PA, USA, SAE Tech. Paper 2007-01-0817, 2007.

[16] M. K. Salaani and D. H. Elsasser, "Heavy vehicle hardware-in-the-loop crash avoidance safety system simulation with experimental validation," in *Proc. 25th Int. Tech. Conf. Enhanced Saf. Vehicles (ESV) Nat. Highway Traffic Saf. Admin.*, 2017, pp. 1–8.

[17] J. P. Chrstos and P. A. Grygier, "Experimental testing of a 1994 Ford taurus for NADSdyna validation," SAE Int., Warrendale, PA, USA, SAE Tech. Paper 970563, Feb. 1997.

[18] G. J. Heydinger, M. K. Salaani, W. R. Garrott, and P. A. Grygier, "Vehicle dynamics modelling for the national advanced driving simulator," *Proc. Inst. Mech. Eng., D, J. Automobile Eng.*, vol. 216, no. 4, pp. 307–318, Apr. 2002.

[19] W. Pan and Y. E. Papelis, "Real-time dynamic simulation of vehicles with electronic stability control: Modelling and validation," *Int. J. Vehicle Syst. Model. Test.*, vol. 1, pp. 143–167, Jan. 2005.

[20] J. E. Stellet, M. R. Zofka, J. Schumacher, T. Schamm, F. Niewels, and J. M. Zollner, "Testing of advanced driver assistance towards automated driving: A survey and taxonomy on existing approaches and open questions," in *Proc. IEEE 18th Int. Conf. Intell. Transp. Syst.*, Sep. 2015, pp. 1455–1462.

[21] S. Ulbrich *et al.*, "Testing and validating tactical lane change behavior planning for automated driving," in *Automated Driving*. Cham, Switzerland: Springer, 2017.

[22] *Road Vehicles—Functional Safety*, International Standard ISO/FDIS 26262, I ISO, 2018.

[23] S. Buggaveeti, "Dynamic modeling and parameter identification of a plug-in hybrid electric vehicle," M.S. thesis, Univ. Waterloo, Waterloo, ON, Canada, 2017.

[24] C.-J. Kat and P. S. Els, "Validation metric based on relative error," *Math. Comput. Model. Dyn. Syst.*, vol. 18, no. 5, pp. 487–520, Oct. 2012.

[25] J. Cuadrado, D. Vilela, I. Iglesias, A. Martín, and A. Peña, "A multibody model to assess the effect of automotive motor in-wheel configuration on vehicle stability and comfort," in *Proc. ECCOMAS Thematic Conf. Multibody Dyn.*, 2013, pp. 1083–1092.

[26] A. Pena, I. Iglesias, J. Valera, and A. Martin, "Development and validation of Dynacar RT software, a new integrated solution for design of electric and hybrid vehicles," in *Proc. EVS*, Los Angeles, CA, USA, 2012, pp. 1–7.

[27] A. Kiruthika, A. A. Rajan, and P. Rajalakshmi, "Mathematical modelling and speed control of a sensored brushless DC motor using intelligent controller," in *Proc. IEEE Int. Conf. Emerg. Trends Comput., Commun. Nanotechnol. (ICECCN)*, Mar. 2013, pp. 211–216.

[28] R. Lattarulo, L. González, E. Martí, J. Matute, M. Marcano, and J. Pérez, "Urban motion planning framework based on N-Bézier curves considering comfort and safety," *J. Adv. Transp.*, vol. 2018, pp. 1–13, Jul. 2018.

[29] R. Rajamani, *Vehicle Dynamics and Control* (Mechanical Engineering Series). Boston, MA, USA: Springer, 2012.

[30] C. Flores and V. Milanés, "Fractional-order-based ACC/CACC algorithm for improving string stability," *Transp. Res. C, Emerg. Technol.*, vol. 95, pp. 381–393, Oct. 2018.

[31] B. Houska, H. J. Ferreau, and M. Diehl, "ACADO toolkit—An open-source framework for automatic control and dynamic optimization," *Optim. Control Appl. Methods*, vol. 32, no. 3, pp. 298–312, 2011.

Jose Angel Matute-Peaspan (Member, IEEE) received the Mechanical Engineering and Magister in mechanical engineering degrees from Simon Bolivar University, Venezuela, in 2008 and 2011, respectively. He is currently pursuing the Ph.D. degree with the University of the Basque Country. He has been a Research Engineer with the Automated Driving & Control Research Group, Tecnalia Research & Innovation, since 2017. He is also working with National (Spain) and European Projects related to vehicle motion planning and control for automated driving.

Asier Zubizarreta-Pico graduated in automation and electronics engineering in 2006. He received the Ph.D. degree in robotics and automatic control systems from the University of the Basque Country in 2010. He is currently teaching with the Department of Automatic Control and Systems Engineering, Higher Technical Engineering School in Bilbao, (UPV/EHU). He is one of the academic coordinators of the Formula Student Project Bizkaia.

Sergio E. Diaz-Briceno received the degree in mechanical engineering from Simon Bolivar University (USB), Venezuela, in 1993, and the Ph.D. degree from Texas A&M University in 1999. He was a Full Professor with USB from 1993 to 2018. He was the President of the FUNINDES-USB Research and Development Foundation, the Head of Machinery Dynamics Laboratory, and an Advisor of ASME, SAE, and SOLAR sections. He has been a Researcher of automated driving & control with the Tecnalia Research & Innovation, since 2018. He was a recipient of international awards as the STLE Burt Newkirk Award, the SAE Ralph Teetor Educational Award, and the F-SAE Carroll Smith Mentor's Cup.